



Toolpath Smoothing Based on Controlled NURBS Interpolation

Yuanjie Guo ^a, Jihong Yan ^b and Xingbo Wang ^{a,c*}

^a Department of Mechatronic Engineering, Foshan University, Foshan, China.

^b R and D, GSK CNC Equipment Co., Ltd, Guangzhou, China.

^c Department of Intelligent Manufacture, Guangdong College of Applied Science and Technology, Zhaoqing, China.

Authors' contributions

This work was carried out in collaboration among all authors. All authors read and approved the final manuscript.

Article Information

DOI: 10.9734/JERR/2023/v25i121041

Open Peer Review History:

This journal follows the Advanced Open Peer Review policy. Identity of the Reviewers, Editor(s) and additional Reviewers, peer review comments, different versions of the manuscript, comments of the editors, etc are available here: <https://www.sdiarticle5.com/review-history/110225>

Original Research Article

Received: 09/10/2023

Accepted: 14/12/2023

Published: 18/12/2023

ABSTRACT

Based on cubic non-uniform B-spline curve constrained with tolerance band, a tool path smoothing approach is proposed for the purpose to achieve high-speed and high-precision machining of consecutive short line segments. According to a given tolerance band, the approach calculates the control polygon of the non-uniform cubic B-spline curve to transition the corners of the short line segments and obtains a GC^2 continuous smooth transition for the tool path near the corners. The paper also designs an algorithm to realize the transition procedure. Compared with the reported similar approaches, this paper's approach has advantages in reducing the fluctuations of machining speed and acceleration, enhancing machining quality, and improving the processing efficiency and motion stability of machine tools. This approach is helpful for CNC system development, as well as CAD and CAM.

Keywords: Tool path; Corner transition; B-spline; Tolerance band; GC^2 continuity.

*Corresponding author: Email: 153668@qq.com;

J. Eng. Res. Rep., vol. 25, no. 12, pp. 60-75, 2023

1. INTRODUCTION

Computer Numerical Control (CNC) systems utilize NC codes generated by CAD/CAM software to execute the machining process[1,2,3]. Since CNC systems are developed with embedded systems, such as ARM and STM32, which have much smaller RAM, much lower computational capacity compared to workstations running CAD/CAM systems, it is necessary to enhance computing speed, smoothness, and other related aspects through algorithm for CNC treatment. Currently, most NC codes consist of short line segments and arc segments, although there are CNC systems such as FANUC and Siemens that can deal with the Non-Uniform Rational B-Splines (NURBS) segments. In 3-axis or multi-axis machining, the short line segments are the majority of the machining paths. Due to the corners at the adjacent points of the short line segments, motion control of the machine tools and quality control of the workpiece become thorny because the frequent acceleration and deceleration to meet the needs of machining the parts around the corners increase the frequency of motion conversion and decrease the machining quality. Therefore, smoothing the tool path that contains consecutive line segments has been a research topic in the field of CAD/CAM/CNC.

Early in 2010, PATELOUP et al. [4] used a cubic B-spline with six control points to smooth the planar tool paths composed of the short line segments and circular arcs. In 2011, ZHANG et al. [5] used parametric cubic spline curves to smoothen the corner transitions. In 2012, BI et al. [6] used cubic Bezier curves for transitions to achieve curvature continuity of the corner path. In 2013, Zhao et al. [7] proposed using B-spline curves that satisfy curvature continuity to achieve corner smoothing transitions and provided corresponding transition strategies. In 2017, TANG et al. [8] proposed an optimization method that inserts cubic B-spline curves at adjacent linear positions to obtain an optimal tool position point spline curve that satisfy the error limit condition and maintains third-order continuity at the connection points. In 2022, CAI et al. [9] put forward a tool position adjustment and a C^3 continuous quintic B-spline curve tool path transition algorithm based on the tolerance band constraint. Huang et al. [10] proposed an algorithm for corner transition using B-spline curves with seven control points. By adjusting the positions of the transition curve control vertices

within a tolerance range, the algorithm reduces the maximum curvature and improves machining efficiency. In 2023, Yan et al.[11] proposed a kinematically coordinated corner smoothing method with double asymmetrical transition curves for corner smoothing in five-axis short line segments. This approach enhances the feedrate at corner locations and achieves low acceleration and jerk of the rotary axes.

We have made deep research on each of the methods mentioned above in our research work of developing CNC system of high performance. Unfortunately, we found none of them could meet the needs of our practice. PATELOUP 's method [4] can merely machine 2 dimensions contours, not available for 3-dimensional or more high dimensional cases. ZHANG's method [5] only ensures continuity between the transition curve and short line segments, still unable to avoid the fluctuations of normal acceleration at the adjacent points of the short line segments. BI 's [6] has to solve an optimal problem to obtain appropriate start and end positions of the transition section, consuming a large amount of computation time. Zhao's [7] requires a large computation cost and is difficult to obtain the optimal solution for smoothness error. TANG's [8] is complicated in computing the control points of the transition curve and lacks global transition strategies. Although CAI's method [9] utilizes constraints of the tolerance band to adjust the tool position, to reduce the approximation error of the short line segments, and to realize smooth transition of the tool path, it's using quintic B-spline curves results in higher computational costs.

In mechanical manufacturing processes, it is difficult to achieve a 100% approximation to the data, thus a certain amount of machining error is usually allowed. Considering the wide application of cubic B-spline curves in industry, we accordingly researched an approach using cubic B-spline curve constrained with the tolerance band to generate smooth tool path. The approach can transition the corners of the short line segments, achieving GC^2 continuity smooth transition of the tool path. This paper introduces the details.

The paper comprises five parts. Aside from this introductory part, Section 2 simply presents essential knowledge on B-spline curves, Section 3 introduces our core approach and algorithm, Section 4 demonstrates numerical experiments, and Section 5 concludes the paper.

2. NON-UNIFORM B-SPLINE CURVES

In this whole paper, our mathematical tool is the non-uniform B-spline curve (NURBS) introduced in [12]. Let $P_i (i=0,1,\dots,n)$ be $n+1$ control points,

which form a control polygon $\langle P_0, P_1, \dots, P_n \rangle$, and $U = \{u_0, u_1, \dots, u_p, u_{p+1}, \dots, u_n, u_{n+1}, \dots, u_{n+p}\}$ be a knot vector; then a p th-degree B-spline curve is defined by

$$C(u) = \sum_{i=0}^n N_{i,p}(u)P_i, \quad u_0 \leq u \leq u_{n+p} \tag{1}$$

where $N_{i,p}(u)$ is the p th-degree B-spline basis function defined by (Eq.2).

$$\begin{cases} N_{i,0}(u) = \begin{cases} 1, & \text{if } u_i \leq u < u_{i+1} \\ 0, & \text{otherwise} \end{cases} \\ N_{i,p}(u) = \frac{u-u_i}{u_{i+p}-u_i} N_{i,p-1}(u) + \frac{u_{i+p+1}-u}{u_{i+p+1}-u_{i+1}} N_{i+1,p-1}(u) \\ \frac{0}{0} = 0 \end{cases} \tag{2}$$

When U is taken to be

$$U = \underbrace{\{a, \dots, a\}}_{p+1}, \underbrace{u_{p+1}, \dots, u_n, b, \dots, b}_{p+1} \tag{3}$$

it is called a clamped knot vector resulting in

$$\begin{cases} C(a) = P_0 \\ C(b) = P_n \end{cases} \tag{4}$$

and

$$\begin{cases} C'(a) = \frac{1}{p+1} (P_1 - P_0) \\ C'(b) = \frac{1}{p+1} (P_n - P_{n-1}) \end{cases} \tag{5}$$

The derivative of (1) is

$$\frac{d}{du} C(u) = C'(u) = \sum_{i=0}^{n-1} N_{i,p-1}(u)P_i \tag{6}$$

Eqs (4), (5), and (6) indicate the curve $C(u)$ is C^{p-1} continuous on interval (a,b) and tangent to the control polygon at the first and the last control points, P_0 and P_n . We will utilize this property to construct the transition curve in later sections.

During the machining process along parametric curves, it is essential to consider the variations in parameterizations. Geometric continuity [13] is widely employed as a metric to assess the smoothness of the tool path. GC^2 continuity, a key aspect of geometric continuity, ensures that two consecutive segments exhibit identical tangent units and curvature vectors at their junction. This characteristic effectively mitigates discontinuities in normal acceleration. For this reason, cubic B-spline curves are chosen due to their ability to achieve the lowest degree of GC^2 continuity, making them an optimal choice for maintaining smooth tool paths in the machining process.

3. METHODOLOGY

In this section, we will present the details of our approach to smoothening tool paths and highlight its advantages. We will begin by demonstrating how to construct a transition curve using a cubic B-spline curve, which is constrained within a tolerance band near the corner of two line segments. Furthermore, we will demonstrate a method to precisely control the approximation error of the transition curve by proportionally adjusting the length of its control polygon. Additionally, we will propose a technique to prevent overlaps near two adjacent transition curves, ensuring a seamless connection. Finally, we will introduce a strategy for constructing a complete GC^2 tool path from a series of short line segments. To provide deeper insights, we will compare our approach with alternative methods to highlight its specific advantages.

3.1 Construction of Transition Curves

Assume three data points Q_0 , Q_1 , and Q_2 constitute two adjacent short line segments, as shown in Fig. 1. The lengths of the line segments $\overline{Q_0Q_1}$ and $\overline{Q_1Q_2}$ are denoted by L_0 and L_1 , respectively. Take five control points, P_0 , P_1 , P_2 , P_3 , and P_4 , on $\overline{Q_0Q_1}$ and $\overline{Q_1Q_2}$ to construct a cubic B-spline curve $C(u)$ to be the transitional curve at the corner formed by $\overline{Q_0Q_1}$ and $\overline{Q_1Q_2}$.

The control points $P_i (i = 0, 1, 2, 3, 4)$ are constrained with $Q_1 = P_2$ and $|P_0P_1| = |P_1P_2| = |P_2P_3| = |P_3P_4| = L$, where L indicates the lengths of the edges of the control polygon. Thus, points P_0 , P_2 , and P_4 form an isosceles triangle $\Delta P_0P_2P_4$. The knot vector is set to $U = \{0, 0, 0, 0, 0.5, 1, 1, 1, 1\}$ so that $C(u)$ is symmetric.

Since points P_0, P_1, P_2 and points P_2, P_3, P_4 are collinear with lines $\overline{Q_0Q_1}$ and $\overline{Q_1Q_2}$, respectively, $C(u)$ is C^2 continuous. Meanwhile, it passes through P_0 and P_4 . Therefore, the required smooth transition tool path is formed by the blended curve $\overline{Q_0P_0} + C(u) + \overline{P_4Q_2}$, which is simply denoted by $\overline{Q_0P_0C(u)P_4Q_2}$. It is surely a GC^2 continuous.

3.2 Selection of Control Points

It is seen that the two short line segments $\overline{Q_0Q_1}$ and $\overline{Q_1Q_2}$ directly affect the control polygon of the transition curve $C(u)$. Geometrically, there are three possible relationships, $L_0 < L_1$, $L_0 > L_1$, and $L_0 = L_1$. Then selection of the control points shall be in terms of each case as follows.

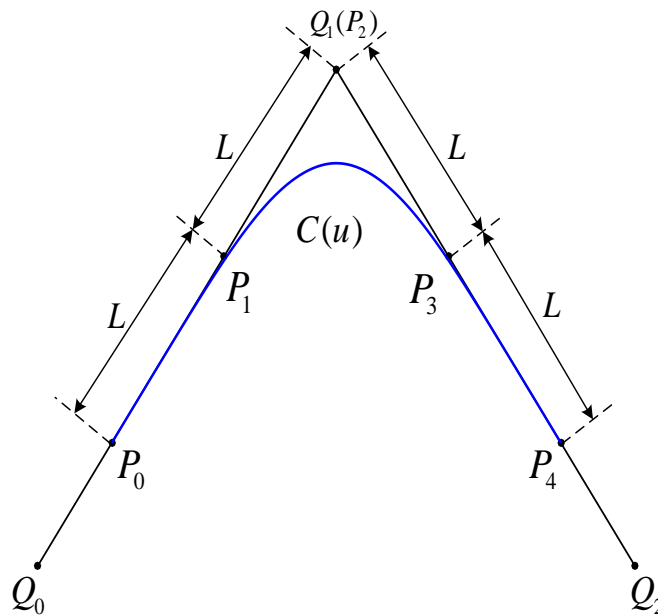


Fig. 1. Transition curve

- (1) If $L_0 < L_1$, let $\beta = \frac{L_0}{L_1}$; then set $P_0 = Q_0$, $P_1 = Q_0 + \frac{1}{2}(Q_1 - Q_0)$, $P_2 = Q_1$, $P_4 = Q_1 + \beta(Q_2 - Q_1)$, and $P_3 = P_2 + \frac{1}{2}(P_4 - P_2)$. Fig. 2(a) illustrates this case. It should be noted that P_1 and P_3 are the midpoints of $\overline{P_0P_2}$ and $\overline{P_2P_4}$, respectively, and that both $\overline{P_0P_2}$ and $\overline{P_2P_4}$ have the same length as L_0 .
- (2) If $L_0 = L_1$, then set $P_0 = Q_0$, $P_1 = Q_0 + \frac{1}{2}(Q_1 - Q_0)$, $P_2 = Q_1$, $P_3 = Q_1 + \frac{1}{2}(Q_2 - Q_1)$, and $P_4 = Q_2$. Fig. 2(b) illustrates this case.
- (3) If $L_0 > L_1$, let $\beta = \frac{L_1}{L_0}$; then set $P_0 = Q_1 + \beta(Q_0 - Q_1)$, $P_2 = Q_1$, $P_1 = P_0 + \frac{1}{2}(P_2 - P_0)$, $P_3 = Q_1 + \frac{1}{2}(Q_2 - Q_1)$, and $P_4 = Q_2$. The case can be seen in Fig. 2(c). P_1 and P_3 are the midpoints of $\overline{P_0P_2}$ and $\overline{P_2P_4}$, respectively, and that both $\overline{P_0P_2}$ and $\overline{P_2P_4}$ have the same length as L_1 .

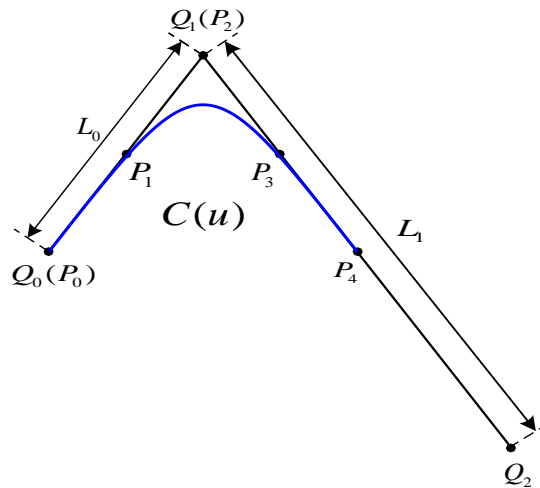


Fig. 2(a). $L_0 < L_1$

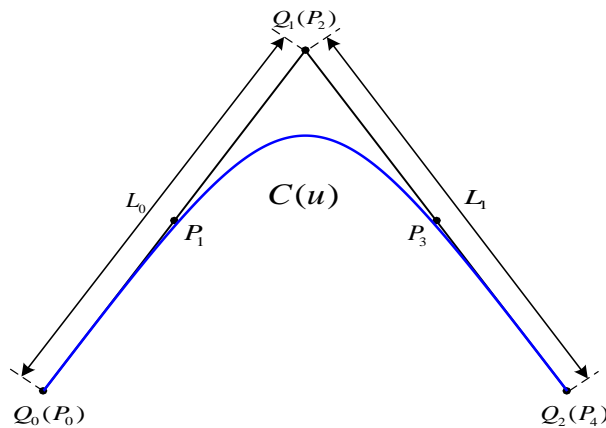


Fig. 2(b). $L_0 = L_1$

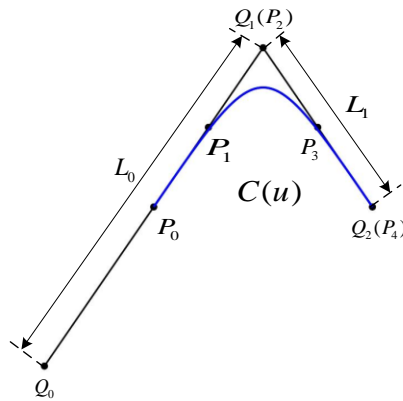


Fig. 2(c). $L_0 > L_1$

Fig. 2. Transitional curves constructed under three conditions

3.3 Controlling of Approximation Errors

The transition curve is ensured to fall within the tolerance band via controlling the approximation error, denoted with symbol e . According to the idea of [6], e is usually estimated by calculating the distance between some sampling points and the original linear tool path. Since the transition curve $C(u)$ is symmetric with respect to the angular bisector of $\overline{P_0P_2}$ and $\overline{P_2P_4}$, e depends on the distance between $Q_1(x_0, y_0, z_0)$ and the shoulder point $C(0.5) = (x_1, y_1, z_1)$ of the transition curve. The calculation is given by

$$e = \sqrt{(x_0 - x_1)^2 + (y_0 - y_1)^2 + (z_0 - z_1)^2} \quad (7)$$

Let 2δ be the permissive tolerance band of the short line tool path, as shown in Fig. 3. Then the distance from the corner of the tolerance band to Q_1 is $\varepsilon = \frac{\delta}{\sin \theta}$, where θ is half the angle at the corner of the short line tool path. Consider adjusting e based on an initial transition curve $C_0(u)$ constructed by means of subsection 3.1. By property of the similar triangle, e is scaled by α times when the control polygon of $C_0(u)$ is enlarged or lessened by α the times. By this means and with a routine described in Fig. 4, we can control e to satisfy $e \leq \varepsilon$ so that the constructed transition curve falls in the tolerance band. In the routine, we need only adjust the value of L to construct a new transition curve until $e \leq \varepsilon$.

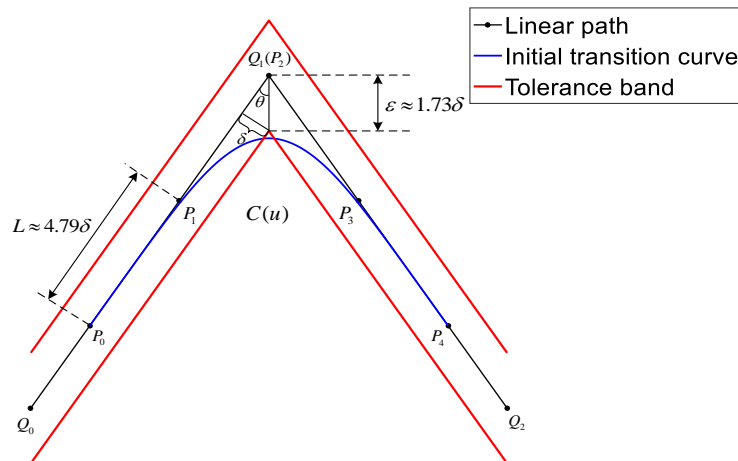


Fig. 3. Construct a tolerance band in figure 1

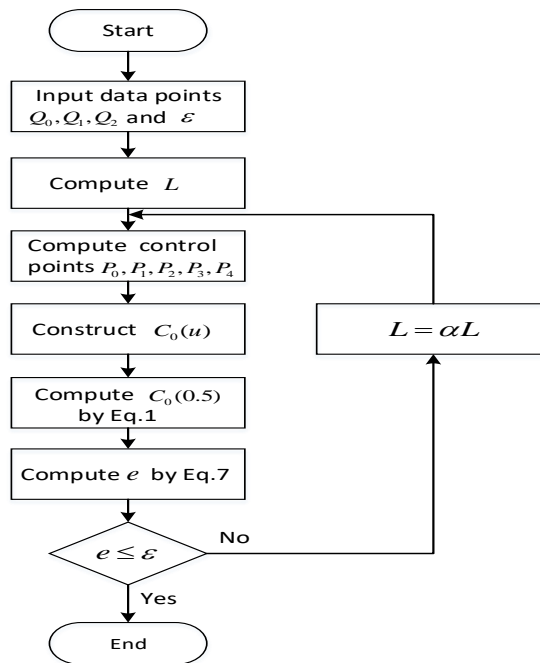


Fig. 4. Computing routine to adjust the approximation error

To make the process clear, we here demonstrate an example of controlling e . Taking the data in Fig. 1 as an example. Suppose the maximum value of δ is set to be $\delta = 0.01mm$; then $\theta = \frac{1}{2} \angle Q_0 Q_1 Q_2 = 35^\circ$ yielding $\varepsilon = \frac{\delta}{\sin \theta} \approx 0.0173mm$. Taking $L \approx 0.0479mm$ results in the initial approximation error of the transition curve $C_0(u)$ is $e_0 \approx 0.0195mm$, saying $C_0(u)$ is out of the tolerance band.

Assume $e^* = \frac{1}{2} \delta = 0.005mm$ is the ideal approximation error; let $\alpha = \frac{e^*}{e_0} = \frac{0.005}{0.0195} \approx 0.256$. Then

keep the control point P_2 unchanged and calculate on $\overline{Q_0 Q_1}$ and $\overline{Q_1 Q_2}$ the new control points P_0^*, P_1^*, P_3^* , and P_4^* such that $L^* = |P_0^* P_1^*| = |P_1^* P_2^*| = |P_2^* P_3^*| = |P_3^* P_4^*| = \alpha L \approx 0.0123mm$. Set the knot vector still by $U^* = \{0, 0, 0, 0, 0.5, 1, 1, 1, 1\}$ and construct a new transition curve $C^*(u)$ as shown in Fig. 5.

This time, a new transition curve $Q_0 P_0^* C^*(u) P_4^* Q_2$ is constructed to satisfy $e^* \approx 0.005mm$. It is surely within the tolerance band and GC^2 continuous.

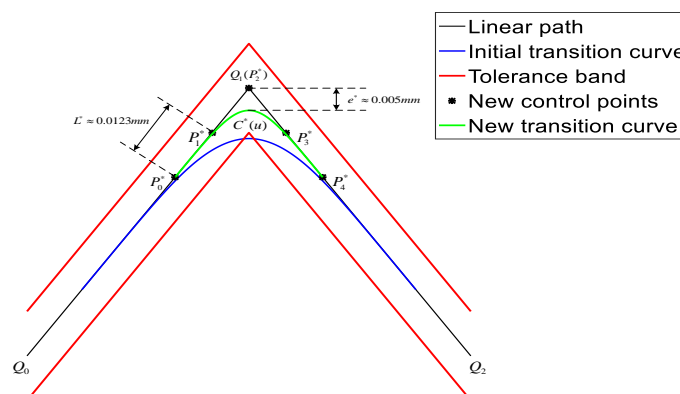


Fig. 5. The new transition curve

3.4 Avoidance of Overlaps

When smoothing the tool path of consecutive short line segments, two neighboring transition curves might be overlapped, as seen In Fig. 6. Such overlap is forbidden in practical machining.

To avoid the overlap, the end-point P_0^e of $C_0(u)$ and the start-point P_1^s of $C_1(u)$ shall be treated to keep a directional distance $d = P_1^s - P_0^e$ such that

$$d = \lambda(Q_2 - P_0^e) \quad 0 \leq \lambda < 1 \quad (8)$$

The value of λ is first determined based on the actual machining, and whenever a transition

curve $C_i(u)$ is constructed, $P_{i+1}^s = P_i^e + \lambda(Q_{i+2} - P_i^e)$ is calculated to construct the next transition curve $C_{i+1}(u)$. Then, if the approximation error of $C_{i+1}(u)$ does not meet the tolerance band constraint, it is made to fall within the tolerance band using the method in subsection 3.3. And if $P_i^e = Q_{i+2}$, a corner point will be formed at Q_{i+2} due to insufficient processing space for the next smooth transition, as shown in Fig. 7. In this case, set $\alpha = \frac{1}{2}$ to adjust the value of the control polygon of $C_i(u)$ to avoid appearing the corner point.

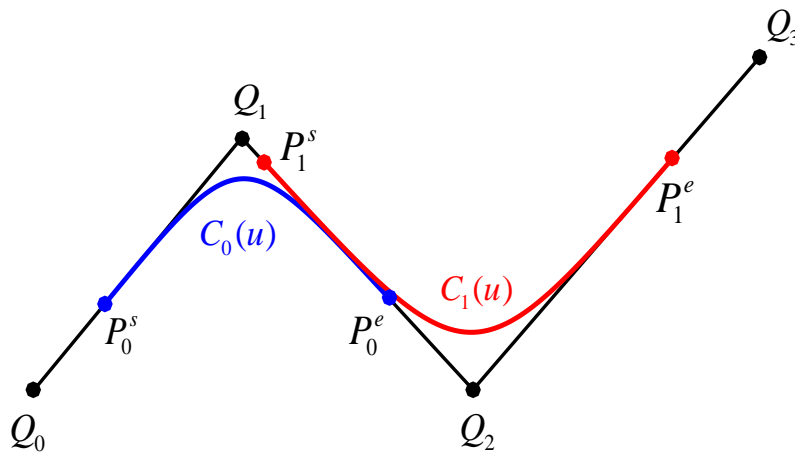


Fig. 6. The overlapping phenomenon between transition curves

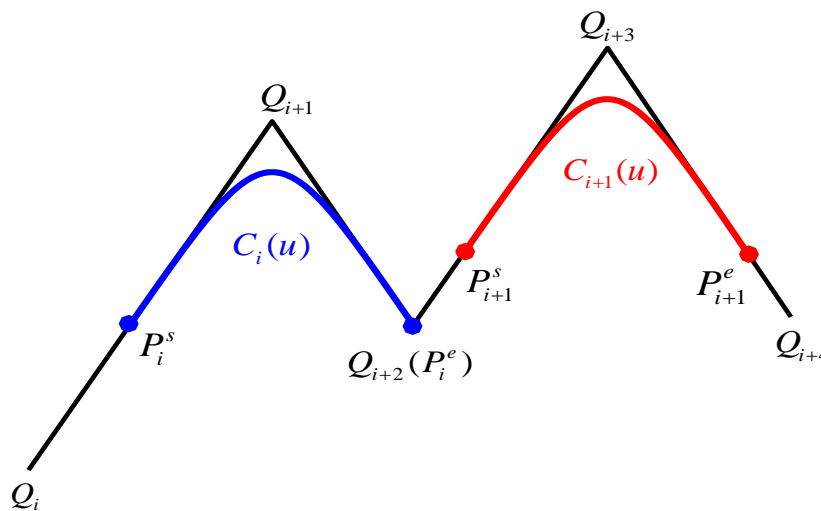


Fig. 7. Corner point at Q_{i+2}

3.5 A Whole GC² Tool Path

Assuming a set of n short line segments with data points $Q_i, i=0,1,\dots,n$, which require $n-1$ transition curves, say $C_i(u), i=0,1,2,\dots,n-2$. Suppose the tolerance band is 2δ and $\varepsilon_i = \frac{\delta}{\sin \theta_i}, i=0,1,2,\dots,n-2$, where ε_i and θ_i are as stated before. Denote e^* to be the ideal approximation error and $e_i, i=0,1,\dots,n-2$, to be respectively the initial approximation errors for

$C_i(u)$, and $L_i, i=0,1,2,\dots,n-2$ to be the edge length of $C_i(u)$'s control polygon; let $\alpha_i = \frac{e^*}{e_i}, i=0,1,2,\dots,n-2$ be the ratio to control the approximation error and λ be the value set to avoid the overlap of transition curves.

For convenience, we use symbol $A \Rightarrow B$ to mean calculating B from A. The whole GC² tool path within the tolerance 2δ is constructed by following three routines.

Routine 1: Process the first three points.

Step 1:

$$Q_0, Q_1, Q_2 \Rightarrow \begin{cases} \theta_0, \varepsilon_0 = \frac{\delta}{\sin \theta_0} \\ < P_0^0, P_1^0, P_2^0, P_3^0, P_4^0 > \end{cases} \text{ with } L_0 = |P_0^0 P_1^0| = |P_1^0 P_2^0| = |P_2^0 P_3^0| = |P_3^0 P_4^0|.$$

$$\text{Step 2: } < P_0^0, P_1^0, P_2^0, P_3^0, P_4^0 > \Rightarrow \begin{cases} C_0(u) \\ e_0 = |P_2^0 C_0(0.5)| \end{cases}$$

Step 3: If $e_0 > \varepsilon_0$, then

$$< P_0^0, P_1^0, P_2^0, P_3^0, P_4^0 > \Rightarrow < P_0^{0*}, P_1^{0*}, P_2^{0*}, P_3^{0*}, P_4^{0*} > \Rightarrow C_0^*(u) \text{ , with } L_0^* = |P_0^{0*} P_1^{0*}| = |P_1^{0*} P_2^{0*}| = |P_2^{0*} P_3^{0*}| = |P_3^{0*} P_4^{0*}| = \alpha_0 L_0.$$

Otherwise (namely, $e_0 \leq \varepsilon_0$), for case $P_4^0 = Q_2$ set $L_0^* = |P_0^{0*} P_1^{0*}| = |P_1^{0*} P_2^{0*}| = |P_2^{0*} P_3^{0*}| = |P_3^{0*} P_4^{0*}| = \frac{1}{2} L_0$, and for the case $P_4^0 \neq Q_2$ designate P_4^0 to be P_4^{0*} of the next transition curve if needed.

Fig. 8 is to describe the whole routine.

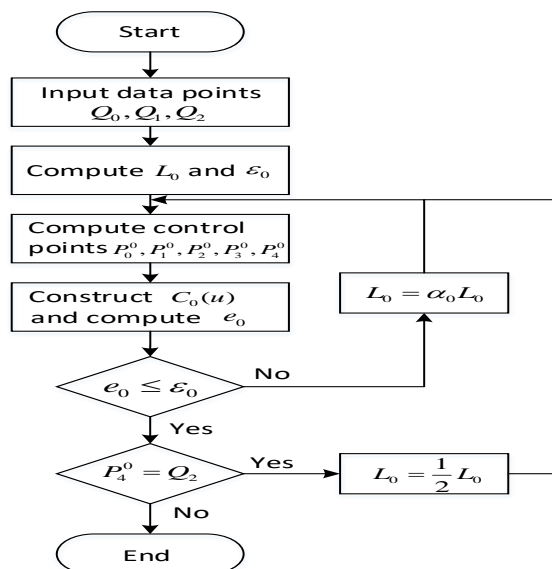


Fig. 8. Flowchart of Routine 1

Routine 2: Processing the intermediate points.

Step 1:

$$P_0^1 = P_4^{0*} + \lambda(Q_2 - P_4^{0*}).$$

Step 2:

$$P_0^1, Q_2, Q_3 \Rightarrow \begin{cases} \theta_1, \varepsilon_1 = \frac{\delta}{\sin \theta_1} \\ \langle P_0^1, P_1^1, P_2^1, P_3^1, P_4^1 \rangle \end{cases} \quad \text{with } L_1 = |P_0^1 P_1^1| = |P_1^1 P_2^1| = |P_2^1 P_3^1| = |P_3^1 P_4^1|.$$

Step 3:

$$\langle P_0^1, P_1^1, P_2^1, P_3^1, P_4^1 \rangle \Rightarrow \begin{cases} C_1(u) \\ e_1 = |P_2^1 C_1(0.5)| \end{cases}$$

Step 4:

If $e_1 > \varepsilon_1$, then

$$\langle P_0^1, P_1^1, P_2^1, P_3^1, P_4^1 \rangle \Rightarrow \langle P_0^{1*}, P_1^{1*}, P_2^{1*}, P_3^{1*}, P_4^{1*} \rangle \Rightarrow C_1^*(u), \text{ with } L_1^* = |P_0^{1*} P_1^{1*}| = |P_1^{1*} P_2^{1*}| = |P_2^{1*} P_3^{1*}| = |P_3^{1*} P_4^{1*}| = \alpha_1 L_1.$$

Otherwise (namely, $e_1 \leq \varepsilon_1$), for case $P_4^1 = Q_3$ set $L_1^* = |P_0^{1*} P_1^{1*}| = |P_1^{1*} P_2^{1*}| = |P_2^{1*} P_3^{1*}| = |P_3^{1*} P_4^{1*}| = \frac{1}{2} L_1$, and for the

case $P_4^1 \neq Q_3$ designate P_4^1 to be P_4^{1*} of the next transition curve if needed.

Step 5: Repeat Step 1~4 from Q_4 until Q_{n-1} is reached.

Fig. 9 is to describe the whole routine.

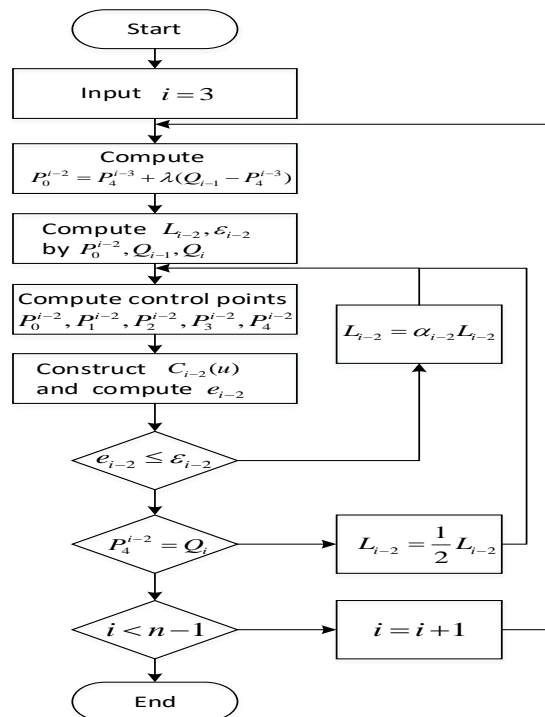


Fig. 9. Flowchart of Routine 2

Routine 3: Processing the endpoint.

Step 1:

$$P_0^{n-2} = P_4^{(n-3)*} + \lambda(Q_{n-1} - P_4^{(n-3)*}).$$

Step 2:

$$P_0^{n-2}, Q_{n-1}, Q_n \Rightarrow \begin{cases} \theta_{n-2}, \varepsilon_{n-2} = \frac{\delta}{\sin \theta_{n-2}} \\ \langle P_0^{n-2}, P_1^{n-2}, P_2^{n-2}, P_3^{n-2}, P_4^{n-2} \rangle \end{cases} \quad \text{with}$$

$$L_{n-2} = |P_0^{n-2} P_1^{n-2}| = |P_1^{n-2} P_2^{n-2}| = |P_2^{n-2} P_3^{n-2}| = |P_3^{n-2} P_4^{n-2}|.$$

Step 3:

$$\langle P_0^{n-2}, P_1^{n-2}, P_2^{n-2}, P_3^{n-2}, P_4^{n-2} \rangle \Rightarrow \begin{cases} C_{n-2}(u) \\ e_{n-2} = |P_2^{n-2} C_{n-2}(0.5)| \end{cases}$$

Step 4:

If $e_{n-2} > \varepsilon_{n-2}$, then

$$\langle P_0^{n-2}, P_1^{n-2}, P_2^{n-2}, P_3^{n-2}, P_4^{n-2} \rangle \Rightarrow \langle P_0^{n-2*}, P_1^{n-2*}, P_2^{n-2*}, P_3^{n-2*}, P_4^{n-2*} \rangle \Rightarrow \langle C_{n-2}^*(u) \rangle,$$

$$\text{with } L_{n-2}^* = |P_0^{n-2*} P_1^{n-2*}| = |P_1^{n-2*} P_2^{n-2*}| = |P_2^{n-2*} P_3^{n-2*}| = |P_3^{n-2*} P_4^{n-2*}| = \alpha_{n-2} L_{n-2}.$$

Fig. 10 is to describe the whole routine.

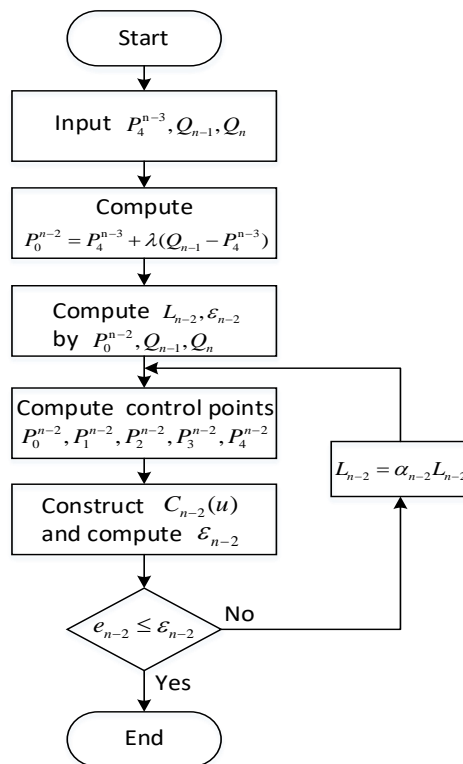


Fig. 10. Flowchart of Routine 3

By such means, a group of short line segment tool paths can be transformed into a GC^2 continuous path constraint with the tolerance band. Fig. 11 shows an example of 4 short line segments. In the figure, the newly-generated tool path is a mixed path consisting of reasonably connected short line segments and B-spline curves $C_0(u)$, $C_1(u)$ and $C_2(u)$.

3.6 Advantages of the Algorithm

Compared with the methods reported in [5-9], our approach exhibits several advantages:

1. Better smoothness. The method in [5] guarantees only C^1 continuity between the transition curve and the short line segment, ours can generate a globally GC^2 continuous smooth tool path.
2. Less computation. The method in [6] has to solve an optimal problem to obtain appropriate start and end positions of the transition section, consuming a large amount of computation time. The method in [9] uses quintic B-spline curves and that in [8] requires calculation of the first and the second derivatives of the cubic B-spline curve to constrain the boundary conditions. They surely need more computation than ours.
3. Easier control of the approximation error. The method in [7] uses adaptive binary to adjust the transition curve to meet the given approximation error and curvature.

Except for a large computational cost, it is not easy to implement in programming. Our method ensures precise approximation error control through proportional adjustments to the control polygon of the transition curve, thereby enhancing implementation simplicity.

4. NUMERICAL SIMULATION

This section exhibits the effectiveness of our approach by using 2-D tool paths and 3-D tool paths.

4.1 D Cases

We use the butterfly-shaped profile comprising 80 short line segments, illustrated in Fig. 12(a). With a tolerance band $\delta = 0.05mm$, we achieve the smooth transitions. Fig. 12(b) is the effectiveness at the corners marked with the square in Fig. 12(a). It is seen that the smooth transitions are within the tolerance band.

4.2 D Cases

We use a closed 3-dimensional hexagon with connection points $Q_i, i = 0, 1, \dots, 6$, as shown in Fig. 13(a) (depicted by the blue solid line). By setting a tolerance band $\delta = 0.05mm$, we obtain five transition curves, $C_i(u), i = 0, 1, 2, 3, 4$. We also obtain the curvature profiles of the five transition curves and show them in Fig. 13(b).

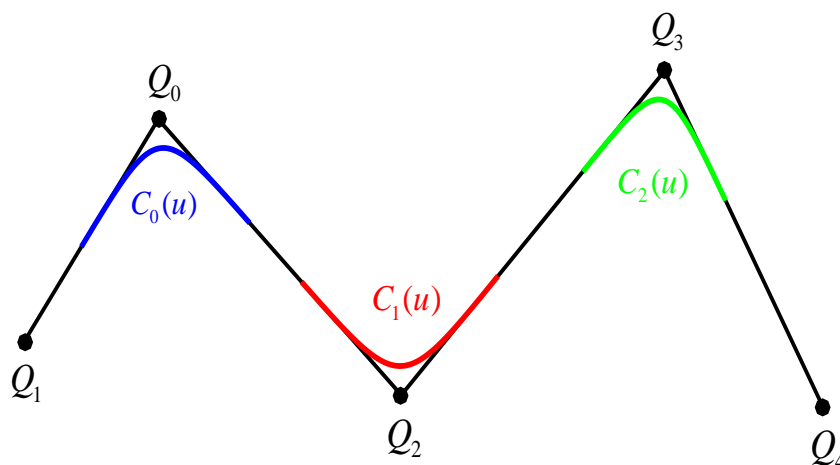


Fig. 11. Application of the algorithm in 4 short line segments

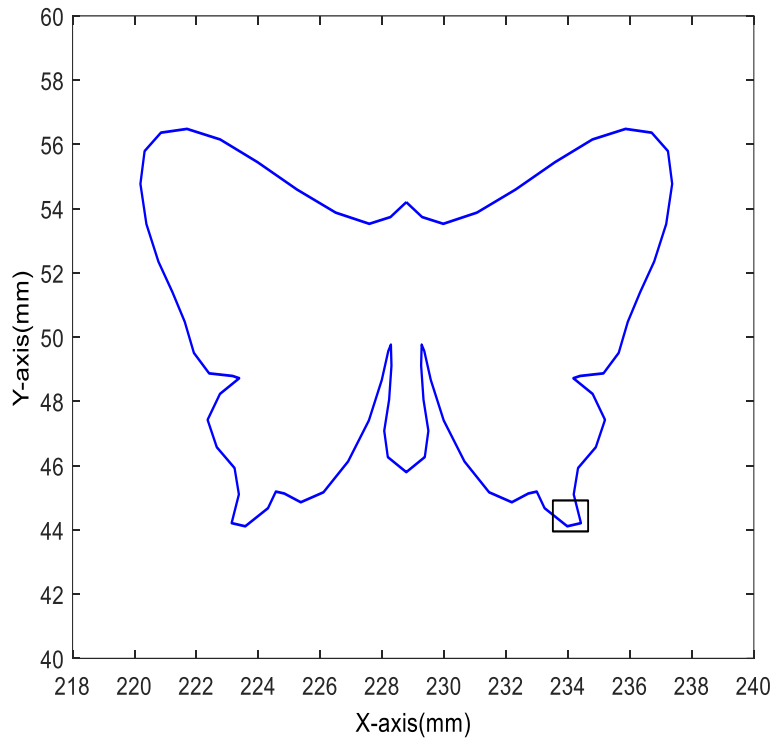


Fig. 12(a). butterfly-shaped profile

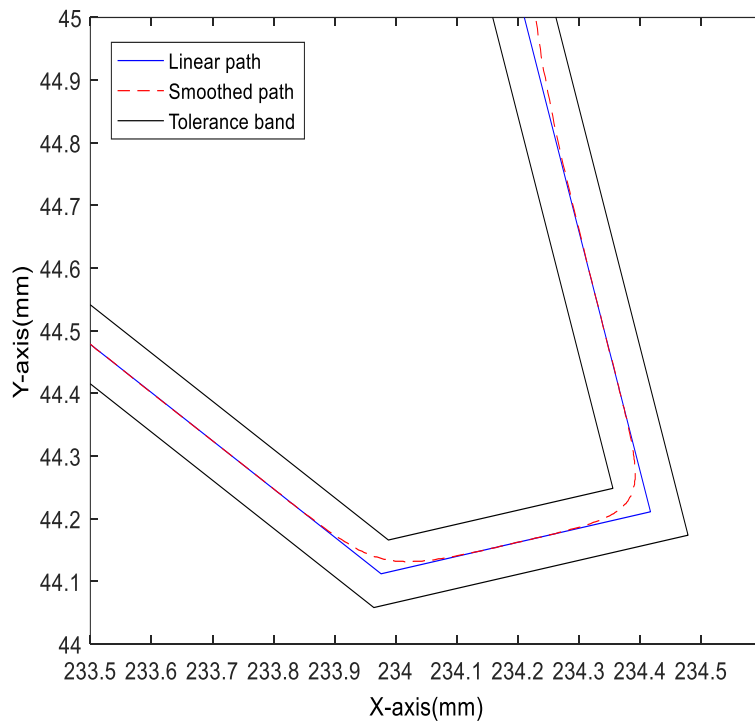


Fig. 12(b). smoothed result

Fig. 12. 2-D tool path for experimental validation

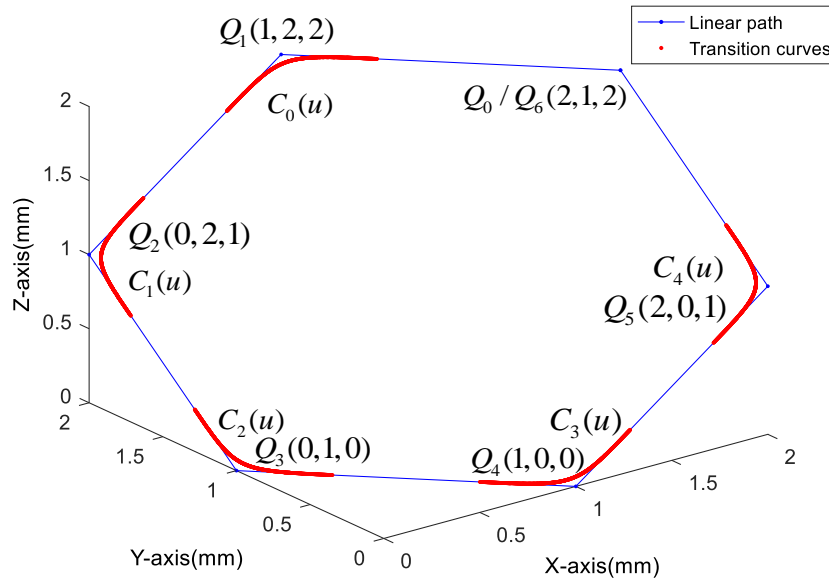


Fig. 13(a). 3-D linear path and transition curves

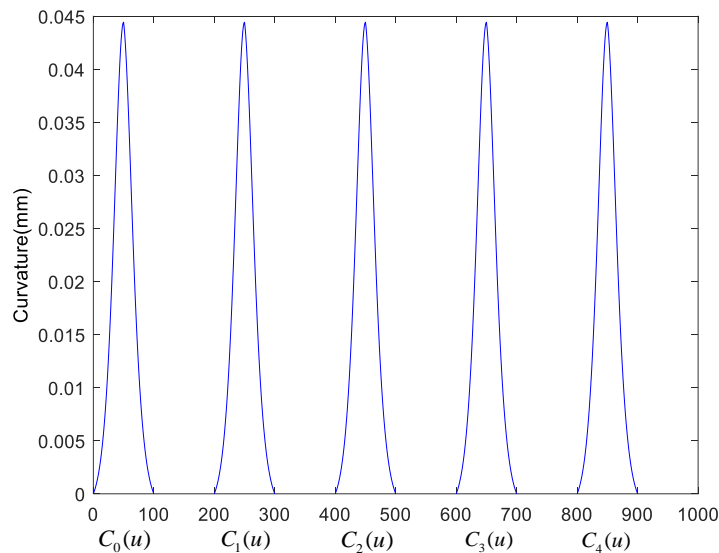


Fig. 13(b). The curvature profiles of the five transition curves

Fig. 13. 3-D tool path for experimental validation

Seen in Fig. 13, the cubic B-spline transition curves are consistently smooth and exhibit uniform curvature. These results indicate that our approach successfully achieves GC^2 continuity for smooth transitions in short line segment tool paths. Being smooth and GC^2 continuity, the transition curves surely have better motion performance than the line segments.

5. CONCLUSION

In order to avoid the feedrate fluctuations and acceleration oscillations that are caused by the discontinuities of tangency and curvature existing in the short line tool path, CNC developers have tried to obtain smooth tool path. Facing the problems existed in the many reported literatures, we made our own researches to meet

the needs of our development and gained the approach introduced in this paper. Experiments show our approach demonstrates expected performance. We hope it helpful for the CAD/CAM/CNC developers in the world.

However, this algorithm still unavoidably has the drawbacks linked to local corner smoothing, such as high computational complexity, large resulting data size that cannot be effectively compressed, and the inability to achieve curvature continuity along the entire toolpath. Exploring optimization strategies for the algorithm to overcome these limitations is a key direction for future research in local corner smoothing methods.

ACKNOWLEDGEMENTS

The authors thanks GSK CNC co., ltd for her supports that enables a series projects for the research work.

COMPETING INTERESTS

Authors have declared that they have no known competing financial interests OR non-financial interests OR personal relationships that could have appeared to influence the work reported in this paper.

REFERENCES

1. Yunwen Sun, Jinjie Jia, Jinting Xu, Mansen Chen, Jinbo Niu. Path, feedrate and trajectory planning for free-form surface machining: A state-of-the-art review. Chinese Journal of Aeronautics. 2022;35(8):12-29. Available:https://doi.org/10.1016/j.cja.2021.06.01
2. Jinting Xu, Dayuan Zhang, Yuwen Sun. Kinematics performance oriented smoothing method to plan tool orientations for 5-axis ball-end CNC machining. International Journal of Mechanical Sciences. 2019;157-158:293-303. Available:https://doi.org/10.1016/j.cja.2021.06.011
3. Jinbo Niu, Jinting Xu, Fei Ren, Yuwen Sun, Dongming Guo. A short review on milling dynamics in low-stiffness cutting conditions: Modeling and analysis. The International Journal of Advanced Manufacturing Technology. 2021;1(1):2020004. Available:https://doi.org/10.51393/j.jamst.2020004
4. Vincent Pateloup, Emmanuel Duc, Pascal Ray. B-spline approximation of circle arc and straight line for pocket machining. Computer-Aided Design. 2010;42:817-827. Available:https://doi.org/10.1016/j.cad.2010.05.003
5. Libing Zhang, Youpeng You, Jun He, Xuefeng Yang. The transition algorithm based on parametric spline curve for high-speed machining of continuous short line segments. The International Journal of Advanced Manufacturing Technology. 2011;52:245-254. Available:https://doi.org/10.1007/s00170-010-2718-z
6. Qingzhen Bi, Yongqiao Jin, Yuhan Wang, et al. An analytical curvature-continuous Bézier transition algorithm for a linear tool path. International Journal of Machine Tools and Manufacture. 2012; 57:55-65. Available:https://doi.org/10.1016/j.ijmactools.2012.01.008
7. Huan Zhao, Limin Zhu, Han Ding. A real-time look-ahead interpolation methodology with curvature-continuous B-spline transition scheme for CNC machining of short line segments. International Journal of Machine Tools & Manufacture. 2013; 65: 88-98. Available:https://doi.org/10.1016/j.ijmactools.2012;10:005
8. Qingchun Tang, Zhiqing Wu, Kehui Li. Research on the Method of Smooth Transition of Local Tool Path. Machine Tool & Hydraulics. 2017;45(4): 18-20,25. Available:https://doi.org/10.3969/j.issn.1001-3881.2017.04.005
9. Anjiang Cai, Feibiao Pang, Juannan Wu. Research on High Precision Machining Methods for Complex Curved Contours, Machinery Design & Manufacture. 2022;378(8):133-136,141. Available:https://doi.org/10.19356/j.cnki.1001-3997.2022.08.015
10. Nuodi Huang, Li Hua, Xi Huang, Yang Zhang, et al. B-spline-based corner smoothing method to decrease the maximum curvature of the transition curve. Journal of Manufacturing Science and Engineering. 2022;144(5):054503. Available:https://doi.org/10.1115/1.4052708
11. Guangwen Yan, Jinlong Liang, Jinting Xu. Overlap classification-based and kinematically coordinated corner rounding using

double asymmetrical transitions for five-axis short-segmented tool path. Journal of Manufacturing Processes. 2023;85:1077-1095.

Available:<https://doi.org/10.1016/j.jmapro.2022.12.018>

12. Les Piegl, Wayne Tiller. The NURBS book. Berlin: Springer Verlag; 1997.

13. Brian Barsky, Tony DeRose. Geometric continuity of parametric curves, University of California at Berkeley, Technical Report 84/205;1984.

© 2023 Guo et al.; This is an Open Access article distributed under the terms of the Creative Commons Attribution License (<http://creativecommons.org/licenses/by/4.0>), which permits unrestricted use, distribution, and reproduction in any medium, provided the original work is properly cited.

Peer-review history:

The peer review history for this paper can be accessed here:

<https://www.sdiarticle5.com/review-history/110225>